Eur. Phys. J. A (2019) **55**: 200
DOI 10.1140/epja/i2019-12893-0

THE EUROPEAN PHYSICAL JOURNAL A

Regular Article – Experimental Physics

Measurement of the $^{13}C(n,\gamma)$ thermal cross section via neutron irradiation and AMS

T. Wright[1,a], S. Bennett[1], S. Heinitz[2,b], U. Köster[3], R. Mills[4], T. Soldner[3], P. Steier[5], A. Wallner[6], and T. Wieninger[5]

[1] University of Manchester, Manchester, UK
[2] Paul Scherrer Institut (PSI), Villigen, Switzerland
[3] Institut Laue-Langevin, Grenoble, France
[4] National Nuclear Laboratory, Seascale, UK
[5] Universität Wien, Wien, Austria
[6] Australian National University, Canberra, Australia

Received: 23 July 2019 / Revised: 6 September 2019
Published online: 14 November 2019

Communicated by P. Woods

Abstract. Ampoules of amorphous 99.5% enriched ^{13}C were irradiated at the PF1b neutron beam line at the high-flux ILL research reactor in order to produce ^{14}C atoms. The precise ratio of $^{14}C/^{13}C$ was subsequently measured at the VERA Accelerator Mass Spectrometer, allowing the $^{13}C(n,\gamma)^{14}C$ thermal cross section to be accurately determined. This is the first measurement of this cross section at sub-eV energies via this technique and the result of 1.52 ± 0.07 mb for the thermal cross section is in good agreement with other recent measurements which were performed via Prompt Gamma-ray Activation Analysis.

1 Introduction and motivation

Accelerator mass spectrometry (AMS) offers a highly sensitive method for determining the number of nuclear reactions that have occurred in certain suitable cases and is therefore being used more frequently to extract accurate cross sections for these reactions. The ^{13}C neutron absorption cross section is particularly suitable for being measured by this technique due to the wealth of experience through the use of AMS for carbon dating. This cross section is of importance to both nuclear energy applications [1,2] and the slow neutron capture process in nuclear astrophysics [3]. The former is mostly concerned with the cross section at low neutron energies (meV to eV), the latter at tens of keV. A recent measurement using AMS focussed on the cross section at keV energies and thus the astrophysical implications [3] and demonstrated clearly the suitability of these techniques for measuring the ^{13}C neutron absorption cross section. Here, the thermal cross section has been measured which has implications for nuclear energy applications, in the context of waste nuclear graphite.

Graphite has historically been used as a neutron moderator due to its high scattering but low absorption neutron cross sections. The first nuclear reactor to achieve criticality, Chicago Pile-1, did so in 1942 with graphite bricks as the moderator and the concept was subsequently commercialised leading to multiple graphite moderated reactors in use across Europe, Asia and North America. The United Kingdom in particular embraced graphite as a moderator and used it extensively; initially for Magnox reactors and later for Advanced Gas-cooled Reactors (AGRs). Currently in the UK, irradiated graphite makes up 23% of the intermediate level nuclear waste, amounting to a volume of approximately 67,000 m^3 weighing 83,000 metric tonnes with a further 14,000 tonnes classed as low level nuclear waste [4]. This nuclear graphite is natural carbon containing 1.1% ^{13}C. After capturing a neutron, the radioisotope ^{14}C is produced which decays via β^- radiation to ^{14}N with a half-life of 5730 ± 40 years [5]. ^{14}C is a radionuclide that can be incorporated into the biosphere and is of concern to nuclear regulators; to decommission and manage waste nuclear graphite in a cost-effective and safe manner, one must know how much ^{14}C is present. To avoid expensive destructive measurement techniques, one relies on the nuclear data for the four main production routes; $^{13}C(n,\gamma)^{14}C$, $^{14}N(n,p)^{14}C$, $^{17}O(n,\alpha)^{14}C$ and $^{18}O(n,n'\alpha)^{14}C$ in order to predict the amount of ^{14}C present in irradiated graphite.

2 Current data

The available data on the $^{13}C(n,\gamma)$ cross section is summarised in table 1. All but the oldest measurement used

[a] e-mail: tobias.wright@manchester.ac.uk
[b] *Present address:* SCK, Belgium.

Table 1. Current data for the thermal ^{13}C neutron capture cross section.

Reference	σ_{thermal} (mb)	Measurement type
Hennig (1954) [6]	0.9 ± 0.2	Activation and chemical separation
Bartholomew (1961) [7]	0.8 ± 0.2	PGAA
Motz (1963) [8]	1.0 ± 0.2	PGAA
Mughabghab (1982) [9]	1.37 ± 0.04	PGAA
Firestone (2016) [10]	1.496 ± 0.018	PGAA

Prompt Gamma-ray Activation Analysis (PGAA), detecting the 8.17 MeV γ-ray from the de-excitation of $^{14}C^{\star}$ formed after ^{13}C absorbs a neutron and normalising to the 2.2 MeV γ-ray from $^{2}H^{\star}$ which is present in a known quantity due to use of a stoichiometric sample. The previously measured values are discrepant; over time, however, uncertainties have decreased as knowledge of the ^{14}C and ^{2}H level schemes have improved along with improvements in detection apparatus leading to the most recent data from [10] having an uncertainty of $\sim 1\%$. The major evaluated nuclear data libraries (ENDF/B-VII, JENDL/D-2017 and TENDL 2017) all take this value whereas JEFF-3.3 uses the slightly lower value from [9]. Given the discrepancies between measured values, the most precise of which use the same measurement technique, and the importance of this cross section, there is strong motivation for a complementary measurement utilising a different experimental approach. Neutron activation and subsequent AMS analysis, as introduced in sect. 1, has no reliance on the decay schemes of ^{14}C and ^{2}H and thus offers an opportunity for a precise independent measurement.

3 Sample preparation

Samples of amorphous 99.5% enriched ^{13}C graphite powder were purchased from Sigma Aldrich and were prepared for the measurement by removing impurities and sealing in quartz ampoules. The other main production route of ^{14}C in irradiated graphite is $^{14}\text{N}(\text{n},\text{p})^{14}\text{C}$, where the cross section for producing ^{14}C is over one thousand times larger than from $^{13}\text{C}(\text{n},\gamma)^{14}\text{C}$; the presence of trace amounts of the adsorbate ^{14}N in the graphite samples therefore represents a significant source of systematic error if inferring the $^{13}\text{C}(\text{n},\gamma)$ cross section from the measured ^{14}C production cross section. The ^{14}C production from $^{17}\text{O}(\text{n},\alpha)$ is negligible due to the combination of the low natural abundance of this isotope (0.038%) and the small cross section (0.235 b) and finally $^{18}\text{O}(\text{n},\text{n}'\alpha)$ can be ignored due to the high neutron energy threshold for this reaction. The quartz ampoules themselves contain 0.02% of ^{17}O by mass and any produced ^{14}C has a recoil energy of 0.4 MeV and an average longitudinal range of 0.93 μm in quartz, thus some nuclei will implant in the amorphous carbon. The production rate of ^{14}C from this is however three to five orders less than the production rate from $^{13}\text{C}(\text{n},\gamma)$, depending on assumptions made about the distribution of carbon within the ampoule and is thus negligible.

Due to the difficulty in accurately measuring the ^{14}N content of the samples pre-irradiation, the approach of removing all ^{14}N from the samples by heating the carbon powder under vacuum was taken, allowing the nitrogen to escape. Five samples containing between 9 and 99 mg ^{13}C were initially prepared at PSI by heating the graphite within 0.4 cm diameter, 3.5 cm length quartz ampoules with a blow torch to red heat under vacuum before flame sealing. As explained in sect. 6, the nitrogen content of these samples was not verifiable. A second set of samples was therefore prepared under more controlled and stringent conditions. This second batch of five ^{13}C samples, weighing between 12 and 36 mg, was prepared at VERA [11] by baking at 900 °C in quartz ampoules for two hours whilst off-gassing, before furnace sealing. Furthermore, three samples of natural (fossil) carbon weighing between 20 and 36 mg were prepared via this same method at VERA in order to estimate the effectiveness of the nitrogen removal (see sect. 6). This natural carbon had a visibly larger grain size than the enriched ^{13}C. The first and second batches were irradiated and analysed via AMS separately in two different measurements, referred to as experiment one ("a" samples) and experiment two ("b" samples) hereafter. Due to the difference in equipment and slight change in procedure for the two sample production methods, the effectiveness of nitrogen removal is expected to be different; a non-negligible nitrogen content would therefore be made apparent by comparing the equivalent ^{14}C production cross section ($\sigma_{^{13}C_{n,\gamma}} + \sigma_{^{14}N_{n,p}}$) from the two irradiations. Similar equivalent cross sections would indicate either a negligible nitrogen content or, more unlikely, that both methods of nitrogen removal were equally, but not perfectly, effective. Significantly different values would indicate that either one or both methods of removal were not successful. Furthermore, by irradiating natural carbon in experiment two, any ^{14}C production from ^{14}N would be more pronounced due to the natural isotopic reduction by a factor of ~ 100 of ^{14}C produced by ^{13}C. Since the natural carbon and enriched ^{13}C have different material properties, one cannot directly infer the ^{14}N content from just this natural carbon measurement. This does, however, provide valuable reassurance. Details of all the samples used for the measurement are summarised in table 3 and there is further discussion regarding the nitrogen content in sect. 6.

4 Neutron irradiation

For both experiment one and two, the samples were irradiated in the primary casemate of PF1b at the ILL

high-flux research reactor [12,13] (operating at 52.8 and 52.5 MW power respectively), where a thermal equivalent capture flux of $\sim 2 \times 10^{10}$ neutrons/cm^2/s with a mean energy of 4 meV is achieved with an active area of 120 cm^2. The irradiations were performed within an active area of $\sim 20\,\mathrm{cm}^2$ selected to exclude inhomogeneous regions close to the borders of the neutron guide. Simulations with the McStas code [14–16] show that within the active area, the neutron flux varies by ±1% in the horizontal direction and ±2% in the vertical direction. For experiment one, samples 1-3a were irradiated for a longer period of time than sample 4a in order to produce different ^{14}C/^{13}C ratios to assess any systematic error associated with the AMS ratio measurements. For experiment two, sample 12b was irradiated for a longer period for the same reason. In all cases, the quartz ampoules were held in a 25 μm thick fluorinated ethylene propylene bag, along with various flux monitors which were used to accurately measure the neutron flux at the irradiation position. For experiment one, the samples were also supported on an aluminium plate; this however was found to be unnecessary and therefore not used for experiment two. Two different flux monitors, copper and zirconium, were chosen in order to reduce systematic uncertainties from the associated nuclear data such as natural isotopic abundances, activation cross sections, branching ratios and half-lives. Multiple foils were distributed throughout the irradiation area next to, in front of and behind the carbon samples. It is standard to use gold as a flux monitor for activation measurements, however in this case the high neutron fluence stipulated the use of a sub mg foil which led to difficulties in the mass measurement, possibly due to contaminants electrostatically attaching to the small amount of gold foil. In order to extract the neutron flux, the activity of the irradiated monitors was measured at a low background germanium detector counting station at two different distances from the detector. The thermal equivalent neutron flux ϕ is related to the total activity of an activated isotope immediately after the irradiation, $A_{\mathrm{activation}}$, by

$$\phi = \frac{A_{\mathrm{activation}}}{\alpha n k_\gamma \sigma_{\mathrm{th}}} \frac{1}{1 - e^{-\lambda t_{\mathrm{irr}}}}\,, \tag{1}$$

where α is the natural abundance of the isotope of interest (taken from [17]), n is the total number of atoms in the flux monitor, k_γ is the self-attenuation factor which is 1 for these Zr and Cu foils, σ_{th} is the thermal neutron capture cross-section for the given isotope (taken from [18]), λ is the decay constant of the given activation product and t_{irr} is the irradiation time. The software Genie 2000 was used to calculate the activity[1]. For all the cross sections considered in this work, that is those of the flux monitors, ^{12,13}C and ^{14}N, a $1/v$ dependence on the neutron energy was assumed with a Westcott factor of 1 allowing a thermal equivalent flux to be determined. Table 2 summarises the flux measurements from the activated isotopes from experiments one and two.

Table 2. Measured neutron flux from the flux monitors. See text for further details on the quoted uncertainties.

Activated isotope	# of foils	ϕ ($\times 10^{10}$ n/cm^2/s)
^{64}Cu/a	8	2.24 ± 0.14
^{95}Zr/a	12	1.96 ± 0.21
^{97}Zr/a	12	2.11 ± 0.21
All foils/a	32	2.09 ± 0.15
^{64}Cu/b	2	2.23 ± 0.07
^{95}Zr/b	6	2.17 ± 0.09
^{97}Zr/b	6	2.21 ± 0.11
All foils/b	14	2.20 ± 0.09

As predicted, no statistically significant differences were found between the foils anterior and posterior to the carbon ampoules, neither with regards to the foil positions spatially within the irradiation area. For each activated isotope in the foils, a weighted mean of the flux values from the two measuring positions was taken as the best estimate of the flux for that isotope/foil; this was in order to reduce the effect of the systematic errors associated with the Ge detector calibration at each measuring position. From these values, best estimates for the flux associated with measurements of each isotope were calculated using a mean weighted on total uncertainty (statistical and systematic) and their errors taken as one standard deviation of the measurements included in the average. These values are shown in table 2. The statistical uncertainties on the activity measurements are linked to the duration each activated foil was measured for. For experiment one, these were approximately 6%, 5% and 4% for ^{64}Cu, ^{95}Zr and ^{97}Zr respectively; they were approximately 3%, 3% and 2% for experiment two. For both experiments one and two, the systematic uncertainties from the neutron activation cross sections, decay constants and branching ratios were approximately 0.4%, 3.3% and 3.0% for ^{64}Cu, ^{95}Zr and ^{97}Zr respectively. The final flux values for experiments one and two, labelled "All foils" in table 2, are taken from a weighted average of all individual isotope measurements from all foils; these values are combined with the irradiation times in table 3 to calculate the respective neutron fluence that each graphite sample received. In an improved future experiment, the systematic uncertainty in the flux measurement could be reduced through the use of flux monitors with 0.1% Au in an Al alloy.

5 AMS measurement

The ^{13}C(n, γ) cross section is simply found through

$$\sigma_{^{13}\mathrm{C}_{(n,\gamma)}} = \frac{1}{\phi t_{\mathrm{irr}}} \frac{^{14}\mathrm{C}}{^{13}\mathrm{C}}\,, \tag{2}$$

[1] ^{152}Eu was used for the Ge detector efficiency calibration. Half-lifes, γ-ray energies and intensities I_γ included in the library used were as follows.
^{64}Cu: $\lambda = 1.52 \times 10^{-5}\,\mathrm{s}^{-1}$, $\gamma_1 = 511\,\mathrm{keV}$ and $I_{\gamma_1} = 35.2\%$, $\gamma_2 = 1345.9\,\mathrm{keV}$ and $I_{\gamma_2} = 0.475\%$.
^{95}Zr: $\lambda = 1.25 \times 10^{-7}\,\mathrm{s}^{-1}$, $\gamma_1 = 724.2\,\mathrm{keV}$ and $I_{\gamma_1} = 43.7\%$, $\gamma_2 = 756.7\,\mathrm{keV}$ and $I_{\gamma_2} = 55.3\%$.
^{97}Zr: $\lambda = 1.14 \times 10^{-5}\,\mathrm{s}^{-1}$, $\gamma_1 = 743.4\,\mathrm{keV}$ and $I_{\gamma_1} = 92.8\%$. ^{97}Nb (daughter of ^{97}Zr): $\lambda = 1.60 \times 10^{-4}\,\mathrm{s}^{-1}$, $\gamma_1 = 657.9\,\mathrm{keV}$ and $I_{\gamma_1} = 98.09\%$.

Table 3. Measured AMS isotopic ratios of all samples. The isotopic ratio uncertainties are taken as one standard deviation of the isotopic ratios of all sputter samples associated with a given sample. No uncertainty is given for 12b because only one AMS measurement was made at the end of the experiment in order not to contaminate the apparatus with ^{14}C.

Sample	Mass (mg)	t_{irr} (min)	$^{14}C/^{13}C$ ($\times 10^{-12}$)
^{13}C/1a	9.1	600	1.173 ± 0.021
^{13}C/2a	46.1	600	1.172 ± 0.013
^{13}C/3a	99.1	600	1.199 ± 0.022
^{13}C/4a	33.5	317	0.622 ± 0.010
^{13}C/5a	74.7	0	0.0011 ± 0.0003
^{13}C/6b	20.0	571	1.154 ± 0.025
^{13}C/7b	32.2	571	1.166 ± 0.014
^{13}C/8b	13.2	0	0.0013 ± 0.0007
^{13}C/9b	20.0	0	0.0017 ± 0.0008
^{nat}C/10b	23.4	571	2.41 ± 0.14
^{nat}C/11b	201.5	571	1.86 ± 0.15
^{nat}C/12b	36.0	13833	5150
IAEA C3	–	–	139.9 ± 1.4
IAEA C6	–	–	164.5 ± 1.3
CTW2	–	–	135.5 ± 4.4

where σ, ϕ and $t_{\rm irr}$ are defined in eq. (1) and $\frac{^{14}C}{^{13}C}$ is the isotopic ratio of ^{14}C (produced by the reaction ^{13}C(n, γ)) to ^{13}C, which can be measured accurately via AMS and is independent of the irradiated sample mass.

The irradiated carbon was taken to the Vienna Environmental Research Accelerator (VERA) [11] where samples suitable for AMS were prepared. Ampoules were broken open under normal atmospheric conditions and multiple sub-mg amounts of material were pressed into aluminium sample holders which are held in a sample magazine capable of holding a total of 40 individual samples including "standards" used for calibration, carbon samples used for tuning the accelerator and unirradiated "blanks" for background measurements. A schematic of the relevant components of VERA is shown in fig. 1. The sample magazine is mounted at the start of the accelerator, where each sample is sputtered with a Cs^+ beam; negative carbon ions are extracted, pre-accelerated across a potential of 75 kV and mass selected ($^{12}C^-$, $^{13}C^-$ or $^{14}C^-$) before being injected into the 3 MV tandem accelerator. Here, they are accelerated to the terminal where they traverse a stripper gas and the resulting positive ions are further accelerated. A subsequent analyzing magnet separates the carbon isotopes. The ($^{12}C^{3+}$ and $^{13}C^{3+}$) beams impinge on separate Faraday cups where their current is measured and individual $^{14}C^{3+}$ ions are bent by a further electrostatic analyzer before being detected in an ionization chamber. The irradiated material was first diluted by a factor of ~ 100 by adding stable carbon in order to reduce the levels of ^{14}C

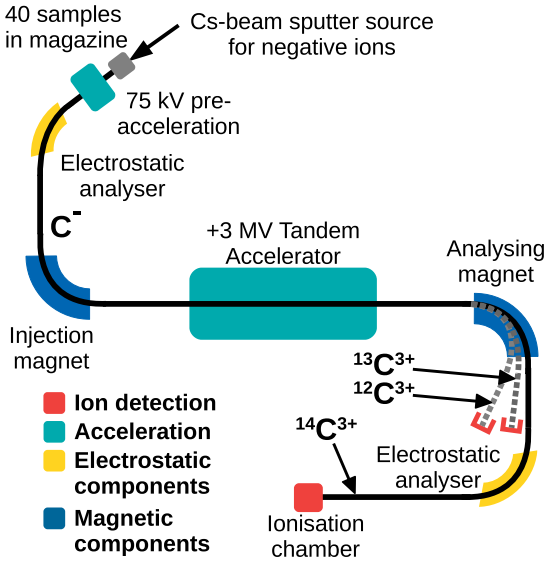

Fig. 1. Schematic of the relevant components of the AMS facility VERA used for this measurement.

present in order to avoid saturating and thus potentially contaminating the apparatus. Once it was confirmed that the carbon isotopic ratios of the diluted samples were the same order of magnitude as those expected, samples of the irradiated material were prepared for measurement.

Each sputter sample within the sample magazine is sputtered for around five minutes during which the AMS setup switches between ^{12}C, ^{13}C or ^{14}C measurements five times per second. In both experiments one and two, the sample magazine contained three sputter samples from each carbon sample (except 12b where only one sputter sample was measured at the end of the run due to its large ^{14}C content, see sect. 6 for details), some "standard" calibration samples containing carbon with well known ($< 1\%$ uncertainty) $^{14}C/^{13}C$ and $^{13}C/^{12}C$ ratios and "old" carbon samples where the ^{14}C has decayed to a negligible amount which are used to periodically tune and thus optimise the detection efficiency of the setup. Each sample is sputtered once per turn of the sample magazine and for experiments one and two there were eight and four turns of the magazine respectively.

The unknown $^{14}C/^{13}C$ ratios are determined by a comparison of the ion currents and count rates to those from the well characterised standard carbon samples; for experiment one, the IAEA C3 and C6 standards were used [19], whereas for experiment two the CTW2 standard was used [20]. The ^{14}C present in the IAEA standards is from natural sources whereas that in the CTW2 originated from irradiating fossil carbon in the Vienna TRIGA reactor and characterizing the resultant material against multiple other standards via AMS. Mean calibration factors, that convert measured isotopic currents and count rates to true isotopic ratios, were found for each periodic tuning of the accelerator. In the unirradiated ^{13}C samples (5a, 8b and 9b) the ^{14}C count rates were 0.09–0.1% of those from the irradiated samples, therefore the contribution of this background to the measured ^{14}C cross section

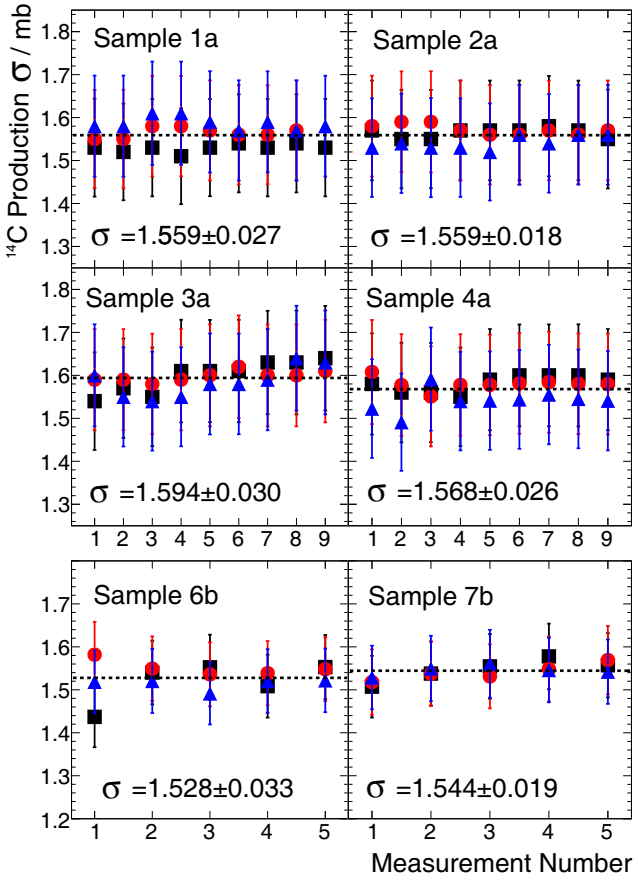

Fig. 2. ^{14}C production cross sections for each carbon sample in the two AMS measurements. Circles, squares and triangles represent the three different sputter samples produced from each carbon sample. The error bars represent the total measurement error: statistical, counting statistics from AMS and systematic, associated with the neutron fluence. The mean values state only the statistical uncertainty.

is negligible. The AMS isotopic ratios for each of the samples are given in table 3 and the resultant ^{14}C production cross sections are shown in fig. 2.

The ^{14}C production cross sections for each of the samples are consistent, as are the repeat measurements. This consistency implies homogeneity throughout the various experimental procedures: sample preparation, irradiation with a constant neutron flux and AMS sputter sample production. The dominant uncertainty from the AMS current and isotope measurement is expected to be statistical and of the order 1–2% [21]; this is confirmed in table 3. As shown in fig. 2, the result of sample 4a is consistent within statistical uncertainties with samples 1-3a suggesting no systematic shifts associated with the AMS measurements.

6 ^{14}N content

A crucial aspect of the analysis is determining how much, if any, ^{14}C originated from ^{14}N(n, p) rather than ^{13}C(n, γ) reactions. The similarity between ^{14}C production cross section measurements shown in fig. 2 suggests that the nitrogen contribution was similar in experiment one and two. Since the samples measured in these measurements were prepared under different laboratory conditions, the agreement implies the nitrogen content is either negligible, or the technique used for the nitrogen removal reached the same saturation limit in both cases. To quantify this, efforts were made to estimate the nitrogen content of the samples. Since ^{14}N does not form a negative ion, it is not possible to directly measure its presence via conventional AMS techniques. This is advantageous due to suppression of the isobaric background in carbon measurements. Furthermore, once the irradiated ampoules are broken open, ^{14}N re-adsorbs to the carbon so measuring the nitrogen content at the point of the AMS measurement is not necessarily indicative of the content during the irradiation phase.

For experiment one, despite these issues, efforts were made to use AMS to estimate the ^{14}N content by following the procedure as described in ref. [3]. This involves mass selecting $A = 27$ which contains the molecule ^{13}C^{14}N$^-$ and measuring the ^{14}N^{3+} counts after the analyzing magnet and thus molecular break up[2]. This eliminates any background from the isobaric compound ^{13}C$_2$^{1}H which does not exist in a charge state $\geq +3$ along with other contaminants such as Al$^-$. In order to compare this value to the ^{13}C content, mass 26 was selected and thus the molecule ^{13}C$_2^-$ was measured giving a quantity proportional to the ^{14}N^{13}C ratio. These measurements were performed for the carbon samples produced for experiment one (samples 1-5a) and the mean ratio was $(7.8 \pm 1.6) \times 10^{-5}$. This ratio, however, cannot be used to directly calculate the ^{14}N content due to the potentially different ionization yields and thus efficiencies for ion extraction by sputtering of ^{13}C^{14}N$^-$ and ^{13}C$_2^-$. In an attempt to correct for this, a stoichiometric compound containing carbon and nitrogen must be measured and for this work sputter samples containing uracil ($C_4H_4N_2O_2$) were prepared and the measured ^{14}N/^{12}C ratio was compared to the true isotopic ratio of 1:1.986. The negative ion yield is affected by the sample matrix and composition, thus various uracil sputter samples were prepared and measured; some diluted with graphite in order to simulate the real targets, and all measurements showed similar ionization yields for $^{12/13}$C$_2^-$ and $^{12/13}$C^{14}N$^-$. Comparing these two currents is therefore sufficiently representative of the ^{14}N/^{13}C ratio for these purposes, suggesting a $\sim$ 78 ppm nitrogen content in the AMS sputter samples prepared from samples 1-5a. It follows that, if this level of nitrogen contamination was present during the ampoules that underwent neutron irradiation, $\sim$ 9.5% of the ^{14}C present after the irradiation would have originated from ^{14}N(n, p). There is however no way to quantify the amount of nitrogen present in the samples during the irradiation or afterwards, during the production of the AMS sputter samples and this value is thus a maximum value for the

[2] $A = 27$ will also contain the molecule ^{12}C^{15}N$^-$ which can be considered negligible in this case due to the high ^{13}C enrichment and low ^{15}N natural abundance.

Table 4. Results for the three irradiated ^{nat}C samples and their inferred nitrogen content.

Sample	^{14}N ppm content
10b	9.7 ± 0.6
11b	5.5 ± 0.6
12b	40800 ± 200

^{14}N content and likely an over-estimate. For this reason, the results from samples 1-5a were not included in the calculation of the ^{13}C(n, γ) cross section.

For experiment two, samples 10-12b of natural carbon were prepared following the same procedure used for the ^{13}C samples and then irradiated in order to produce measurable levels of ^{14}C. For these samples, the production of ^{14}C from ^{13}C is suppressed by a factor of 100 due to the natural isotopic abundance of ^{13}C, such that the ^{14}C content of the irradiated samples will be much more sensitive to the ^{14}N content at the time of irradiation. For example, a natural carbon sample with a nitrogen content of 78 ppm would produce almost a factor of ten more ^{14}C from the ^{14}N(n,p) production route compared to the ^{13}C(n, γ) route. Assuming a similar ^{14}N content in the ^{nat}C and ^{13}C samples after flame sealing (despite their different grain sizes), the best estimate of the fractional nitrogen content with relation to the ^{12}C content is given by

$$N_{^{14}\mathrm{N}} = \frac{1}{\phi t_{\mathrm{irr}} \sigma_{^{14}\mathrm{N}_{(n,p)}}} \left(\frac{N_{^{14}\mathrm{C}}}{N_{^{12}\mathrm{C}}} - \frac{N_{^{13}\mathrm{C}}}{N_{^{12}\mathrm{C}}} \phi t_{\mathrm{irr}} \sigma_{^{13}\mathrm{C}_{(n,\gamma)}} \right), \quad (3)$$

where $N_{^{14}\mathrm{N}}$ is the fractional ^{14}N content, $N_{^{12,13,14}\mathrm{C}}$ are the number of atoms of the relevant carbon isotope, ϕ is the neutron flux found from eq. (1) and σ_x are the relevant thermal capture cross sections; $\sigma_{^{13}\mathrm{C}_{(n,\gamma)}}$ taken from [18] and $\sigma_{^{14}N_{(n,p)}}$ taken from [22]. The results for the natural carbon samples are given in table 4. Although this relies on knowledge of the cross sections *a priori*, which have their own associated uncertainties, the variation in the expected ^{14}N content between samples is dominant when deducing an estimated ^{14}N content.

An 8 ppm ^{14}N content would contribute $\sim 1\%$ to the ^{14}C production in a thermal neutron irradiation of the enriched ^{13}C samples, therefore it is clear from table 4 that the method of sample production was successful in removing nitrogen content to levels within the various other experimental uncertainties for two of the samples. The third sample, however, which was irradiated for ~ 24 times longer contained over 2000 times more ^{14}C, implying a nitrogen content of 4%. This huge difference could perhaps be due to an incomplete flame sealing after the ampoule had been heated.

In summary, these results suggest that the sample production procedure of heating then sealing ampoules of amorphous carbon is able, in most cases, to remove the majority of nitrogen present to levels within the other experimental uncertainties; an unsuccessful attempt at nitrogen remove is made apparent by a drastically larger

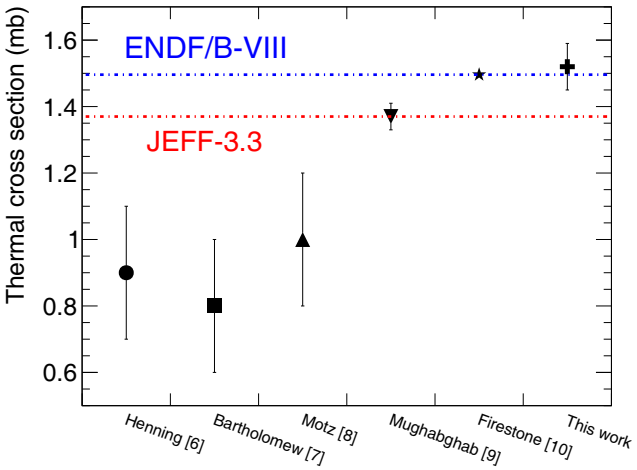

Fig. 3. The measured ^{13}C(n, γ) cross section compared to other measurements and evaluations.

^{14}C content than expected, as was the case for sample 12b. They also confirm that after breaking open the sealed samples, nitrogen adsorbs to the carbon therefore it is impossible to infer the nitrogen content of the irradiated samples after they have been exposed to atmospheric conditions. If the assumption is made that all the carbon samples prepared for experiments one and two have a negligible ^{14}N content and thus all measured ^{14}C is produced from ^{13}C(n, γ), the cross section for this reaction can be calculated using eq. (2). Values for the cross section calculated in this way are shown in fig. 2 for each of the ^{13}C samples. This good agreement is indicative of the nitrogen content being similar in both cases despite the samples being produced separately under slightly different conditions. Leading from this, the nitrogen content can be assumed to be comparable to those measured from the ^{nat}C samples, shown in table 4, and thus the ^{14}N is expected to contribute $(0.93 \pm 0.39)\%$ to the post-irradiation measured ^{14}C for the ^{13}C samples.

7 Results

Only samples 6b and 7b are considered for the cross section calculation and the mean ^{14}C/^{13}C ratio of $(1.159 \pm 0.021) \times 10^{-12}$ is taken from the AMS measurements. This is then divided by the product of the irradiation time (34260 s) and the measured flux for experiment two $((2.20 \pm 0.09) \times 10^{10}$ n/cm^2/s) to give a final ^{14}C production cross section of 1.538 ± 0.069 mb. This value is then reduced by $(0.93 \pm 0.39)\%$ to account for the estimated ^{14}C production from ^{14}N(n, p) to give the final result of $\sigma = 1.52 \pm 0.07$ mb which is compared to other available data in fig. 3. The result is in agreement with the most recent value measured via PGAA [10] which uses fully independent experimental and analytical methods. In the case of PGAA measurements, nitrogen contamination does not pose a problem due to the Q-value of the ^{14}N(n, p)^{14}C reaction (625.9 keV) not being sufficient to result in the emission of the 8.17 MeV γ-ray which is characteristic of

the $^{13}C(n,\gamma)^{14}C$ reaction. A new normalisation was performed in [10] of the results from [9] using more precise data giving a cross section value of 1.502 ± 0.027 mb, also in excellent agreement with the result of this work. The other previous measurement sensitive to nitrogen contamination is of [6]; it is likely here that the nitrogen contribution to the ^{14}C production cross section was overestimated as before subtracting for this, their measured production cross section was 1.5 ± 0.2 mb.

These agreements suggests the nuclear data evaluations should adopt the higher thermal cross section value used in ENDF/B-VIII with confidence. The confirmation of the nuclear data used in the calculations for ^{14}C production in graphite moderated reactors suggest that disagreements between calculated and measured activation levels are likely due to the chosen elemental composition and distribution within the graphite for the calculations rather than the nuclear data. As demonstrated by sample 12b, the natural adsorbant level of ^{14}N in the graphite samples used for this work produces around 50 times more ^{14}C than from the other production routes including $^{13}C(n,\gamma)$. Therefore, it is likely that the nitrogen content in graphite moderated reactors is the most important quantity for the calculation of ^{14}C levels in nuclear graphite, particularly if the reactor core was regularly exposed to air.

8 Summary

Details of the first measurement of the $^{13}C(n,\gamma)$ thermal cross section using neutron irradiation and AMS have been presented and the results confirm the precise values obtained using PGAA giving confidence to nuclear waste calculations carried out using the major evaluations. The use of AMS to directly count the number of transmutated nuclei as a result of a nuclear reaction is further proving to be a sophisticated and complimentary technique for certain cross section measurements. In this particular case, understanding the amount of ^{14}C produced from the $^{14}N(n,p)$ reaction was crucial for success and it has been shown that through a stringent sample preparation procedure, the nitrogen content of the samples has been managed so that its contribution is almost negligible to the final result. The contributing data set to this result with details of all the contributors to the flux and carbon ratios can be found in the corresponding EXFOR entry. The total uncertainty of 4.6% is dominated by the inherent difficulties of measuring the neutron flux over a $\sim 20\,cm^2$ area which in this case was performed with multiple activation foils.

This work was supported by the UK Nuclear Data Network.

Data Availability Statement This manuscript has associated data in a data repository. [Authors' comment: Key data are available within the paper. All data will be uploaded to the EXFOR database, `https://www-nds.iaea.org/exfor/`.]

References

1. W.V. Lensa, D. Vulpius, H.J. Steinmetz, N. Girke, D. Bosbach, B. Thomauske, A.W. Banford, ATW Int. Z. Kernenerg. **56**, 263 (2011).
2. R.W. Mills, Z. Riaz, A.W. Banford, in *Proceedings of the European Nuclear Conference - ENC 2012* (European Nuclear Society, 2012).
3. A. Wallner, M. Bichler, K. Buczak, I. Dillmann, F. Käppeler, A. Karakas, C. Lederer, M. Lugaro, K. Mair, A. Mengoni *et al.*, Phys. Rev. C **93**, 045803 (2016).
4. Tech. rep., ISBN: 978-1-905985-33-3 (2017).
5. F. Ajzenberg-Selove, Nucl. Phys. A **523**, 1 (1991).
6. G.R. Hennig, Phys. Rev. **95**, 92 (1954).
7. G.A. Bartholomew, Annu. Rev. Nucl. Part. Sci. **11**, 259 (1961).
8. H.T. Motz, E.T. Jurney, Washington AEC Office Reports 1044 (1963).
9. S.F. Mughabghab, M.A. Lone, B.C. Robertson, Phys. Rev. C **26**, 2698 (1982).
10. R.B. Firestone, Z. Revay, Phys. Rev. C **93**, 054306 (2016).
11. W. Kutschera, P. Collon, H. Friedmann, R. Golser, P. Hille, A. Priller, W. Rom, P. Steier, S. Tagesen, A. Wallner *et al.*, Nucl. Instrum. Methods B **123**, 47 (1997).
12. H. Häse, A. Knäpfler, K. Fiederer, U. Schmidt, D. Dubbers, W. Kaiser, Nucl. Instrum. Methods A **485**, 453 (2002).
13. H. Abele, D. Dubbers, H. Häse, M. Klein, A. Knäpfler, M. Kreuz, T. Lauer, B. Märkisch, D. Mund, V. Nesvizhevsky *et al.*, Nucl. Instrum. Methods A **562**, 407 (2006).
14. K. Lefmann, K. Nielsen, Neutron News **10**, 20 (1999).
15. P. Willendrup, E. Farhi, K. Lefmann, Physica B **350**, 735 (2004).
16. P. Willendrup, E. Farhi, E. Knudsen, U. Filges, K. Lefmann, J. Neutron Res. **17**, 35 (2014).
17. J. Meija, T.B. Coplen, M. Berglund, W.A. Brand, P. De Bièvre, M. Gröning, N.E. Holden, J. Irrgeher, R.D. Loss, T. Walczyk *et al.*, Pure Appl. Chem. **88**, 293 (2016).
18. S. Mughabghab, *Atlas of Neutron Resonances Resonance Properties and Thermal Cross Sections* (Elsevier, 2018).
19. K. Rozanski, W. Stichler, R. Gonfiantini, E.M. Scott, R.P. Beukens, B. Kromer, J. Van Der Plicht, Radiocarbon **34**, 506 (1992).
20. T. Weininger, Master's Thesis, University of Vienna (2013).
21. M.J. Nadeau, P.M. Grootes, Nucl. Instrum. Methods B **294**, 420 (2013).
22. G.C. Hanna, D.B. Primeau, P.R. Tunnicliffe, Can. J. Phys. **39**, 1784 (1961).